arXiv:0906.2770v1 [cs.CV] 15 Jun 2009

Combinatorial pyramids and discrete geometry for energy-minimizing segmentation

Martin Braure de Calignon†, Luc Brun‡, and Jacques-Olivier Lachaud†

†LaBRI CNRS UMR 5800
Université Bordeaux 1
351, cours de la Libération
33405 Talence cedex
{braure,lachaud}@labri.fr

‡GreyC CNRS UMR 6072
Équipe Image - ENSICAEN
6, Boulevard du Maréchal Juin
14050 CAEN Cedex - France
{luc.brun}@greyc.ensicaen.fr

Abstract. This paper defines the basis of a new hierarchical framework for segmentation algorithms based on energy minimization schemes. This new framework is based on two formal tools. First, a combinatorial pyramid encode efficiently a hierarchy of partitions. Secondly, discrete geometric estimators measure precisely some important geometric parameters of the regions. These measures combined with photometrical and topological features of the partition allows to design energy terms based on discrete measures. Our segmentation framework exploits these energies to build a pyramid of image partitions with a minimization scheme. Some experiments illustrating our framework are shown and discussed.

1 Introduction

The convergence of energy minimization and hierarchical segmentation algorithms provides a rich framework for image segmentation. This framework is based on an objective criterion, called *energy*, whose minimization defines a salient partition according to a given problem . The energy of a partition is generally decomposed by summation over each region as a weighted sum of two terms $E(R) = E_{img}(R) + \nu E_{reg}(R)$ where E_{img} may be understood as a fit to the data within the region while E_{reg} corresponds to a regularization term. The parameter ν defines the respective weights of the two terms. The Mumford-Shah energy is a classical instance of this approach [1]. Such equation may also be interpreted within the Minimum Description Length (MDL) framework [2], where the two energies E_{img} and E_{reg} represent respectively the encoding costs of the photometry and the geometry of a region.

Several methods have been proposed in order obtain a partition minimizing an energy. These methods include the level set approach [1], graph cuts [3] and the methods based on a region merging scheme [4–7]. The definition of a meaningful segmentation using an energy minimization framework and a merge scheme supposes first to define a merge strategy. If the parameter ν is fixed, a near optimal strategy consists to merge at each step the two regions, the merging of which induces the greatest decrease of the energy until any merge would increase the energy. The obtained partition is said to be *2 normal* at the scale

ν [4, 5]. An alternative strategy [6] consists to merge at each step the two regions whose union would belong to the 2 normal partition of lowest scale. This reduction framework avoids the need to select a vector of ν parameters encoding *a priori* the different scales of interest. However, previous works [4–6] where based on a sequence of merge operations combined with a stopping criterion (number of regions, maximal value of $\nu \ldots$). Guigues *et. al.* [7] encode explicitly the hierarchy of partitions using a reduction scheme similar to [6] but uses the hierarchy in order to build for any value of ν, the optimal partition which may be defined from the hierarchy. Moreover, instead of starting from the grid of pixels like [6], their initial partition is an over partition of the image, which presents two fundamental advantages. First, the initial over segmented partition allows to compute reliable statistics on regions. Secondly, it restricts the set of possible partitions and thus reduces the risk to be trapped into a local minima.

The second problem that should be addressed by a segmentation algorithm is the correct design of the energy terms. For instance, the classical Mumford-Shah energy simply combines the squared error of each region together with the total length of the partition boundaries. However, as shown by several authors [7], more complex models (both geometrical and photometrical) may handle finer definitions of salient partitions. Their design requires to fit geometrical models onto regions. An efficient access to the set of boundaries of each region and to their geometry is thus compulsory. However, classical hierarchical segmentation frameworks are not adequate for this task. Adaptive pyramids based on graph [8] do not present a 1-1 correspondence between region adjacencies and geometrical boundaries: reconstructing the geometry of a region is then tricky. Dual graphs [9] behave better for this task but the explicit encoding of all reduced graphs restricts the number of merge steps.

This paper provides a new framework that addresses the design of new energy terms based on geometrical and photometrical features. The stack of successively reduced partitions is encoded using a combinatorial pyramid [10]. A very fine granularity for the hierarchy is then achieved since regions are merged two by two and a new level of the pyramid is created for each merging operation. Geometrical features are computed on each partition of the hierarchy using discrete geometric estimators of normal and length. This framework offers then a compact and efficient encoding of the hierarchy together with an efficient access to the geometrical and topological properties of the partition. It came thus as a natural complement to methods searching for optimal partitions. The paper is structured as follows. We present in Section 2 the combinatorial pyramid model. The application of this model to compute geometrical features on regions using discrete geometric estimators is presented in Section 3. We then present in Section 4 one energy based on discrete estimators together with some experiments.

2 Combinatorial Pyramids

This paper is based on combinatorial maps [11]. A combinatorial map may be seen as a planar graph encoding explicitly the orientation of edges around a

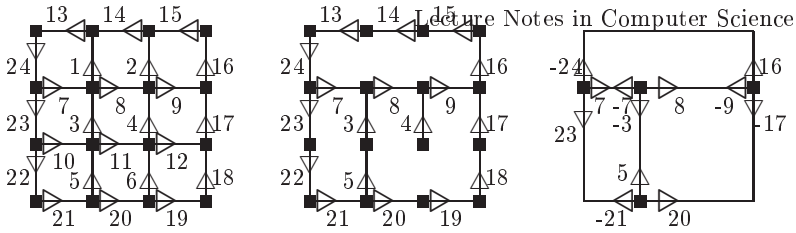

(a) $\overline{G_0}$ (b) $\overline{G_1}$ contracted (c) $\overline{G_3}$ reduced

Fig. 1. A dual of a combinatorial map (a) encoding a 3×3 grid with the contracted combinatorial map (b) obtained by the contraction of the contraction kernel (CK) $K_1 = \alpha^*(1, 2, 10, 11, 12, 6)$. The reduced combinatorial map (c) is obtained by the removal of the empty self loops defined by the RKESL $K_2 = \alpha^*(4)$ and the removal kernel of empty double edges (RKEDE) $K_3 = \alpha^*(13, 14, 15, 19, 18, 22) \cup \{24, -16, 17, -20, 21, -23, 3, -5\}$.

given vertex. To do so, each edge of a planar graph is split into two half-edges called *darts* (e.g. darts 16 and -24 in Fig. 1c). Since each edge connects two vertices, each dart belongs to only one vertex. A combinatorial map is formally defined by a triplet $G = (\mathcal{D}, \sigma, \alpha)$ where $\mathcal{D}$ represents the set of darts and σ is a permutation on $\mathcal{D}$ whose cycles correspond to the sequence of darts encountered when turning counter-clockwise around each vertex. Finally α is an involution on $\mathcal{D}$ which maps each of the two darts of one edge to the other one (e.g. α maps 16 to -24 and -24 to 16 in Fig 1c). The cycles of α and σ containing a dart d will be respectively denoted by $\alpha^*(d)$ and $\sigma^*(d)$.

Given a combinatorial map $G = (\mathcal{D}, \sigma, \alpha)$, its dual map is defined by $\overline{G} = (\mathcal{D}, \varphi, \alpha)$ with $\varphi = \sigma \circ \alpha$. The cycles of permutation φ encode the faces of the combinatorial map and may be interpreted as the sequence of darts encountered when turning clockwise around a face. The cycle of φ containing a dart d will be denoted by $\varphi^*(d)$.

2.1 Combinatorial map encoding of a planar sampling grid

Combinatorial maps can also code the low level geometry of image pixels. Indeed, Fig. 1a describes a dual combinatorial map $\overline{G_0} = (\mathcal{D}_0, \varphi_0, \alpha_0)$ encoding a 3×3 4-connected planar sampling grid. The φ, α and σ cycles of each dart may be respectively understood as elements of dimensions 0, 1 and 2 and formally associated to a 2D cellular complex [10]. More precisely, each α_0 cycle may be associated to a *linel* (sometimes also called *crack* or *surfel*) between two pixels. Each of the two darts of an α_0 cycle corresponds to an orientation along the linel. For example, the cycle $\alpha_0^*(1) = (1, -1)$ is associated to the linel encoding the right border of the top left pixel of the 3×3 grid (Fig. 1a). Darts 1 and -1 define respectively a bottom to top and top to bottom orientation along the linel.

2.2 Construction of Combinatorial Pyramids

A combinatorial pyramid is defined by an initial combinatorial map successively reduced by a sequence of contraction or removal operations. Contraction operations are encoded by contraction kernels (CK). These kernels, defined as a forest of the current combinatorial map, may however create redundant edges such as empty-self loops and double edges. Empty self loops (edge $\alpha_1^*(4)$ in Fig. 1b) may be interpreted as region inner boundaries and are removed by a removal kernel of empty self loops (RKESL) after the contraction step. The remaining redundant edges, called double edges, belong to degree 2 vertices in $\overline{G}$ (e.g. $\varphi_1^*(13)$, $\varphi_1^*(14)$, $\varphi_1^*(15)$) in Fig. 1b) and are removed using a removal kernel of empty double edge (RKEDE) which contains all darts incident to a degree 2 dual vertex. Further details about the construction scheme of a combinatorial pyramid may be found in [10]

As mentioned in Section 2.1, if the initial combinatorial map encodes a planar sampling grid, the geometrical embedding of each initial dart corresponds to an oriented linel. Moreover, each dart of a reduced map that is not a self loop encodes a connected boundary between two regions. The embedding of the boundary associated to such a dart may be retrieved from the embedding of the darts of the initial map G_0. Let us consider the reduced combinatorial map $G_i = (\mathcal{D}_i, \sigma_i, \alpha_i)$ defined at level i and one dart $d \in \mathcal{D}_i$ which is not a self loop. The sequence $d_1 \ldots, d_n$ of initial darts encoding the embedding of the dart d is obtained from the receptive field of d [10] within G_0 using the following relation:

$$d_1 = d \, , d_{j+1} = \underbrace{\varphi_0 \circ \cdots \circ \varphi_0}_{m_j \text{ times}}(\alpha_0(d_j)) \tag{1}$$

where $\overline{G_0} = (\mathcal{D}_0, \varphi_0, \alpha_0)$ is the dual of the initial combinatorial map and m_j is the smallest integer q such that $\varphi_0^q(\alpha_0(d_j))$ survives at level i or belongs to some former RKEDE. The dart d_n is the first dart defined by Eq. (1) which survives up to level i. This dart also satisfies $\alpha_0(d_n) = \alpha_i(d)$ by construction of the receptive fields. Note that the tests performed on $\varphi_0^q(\alpha_0(d_j))$, $q \in \{1, \ldots, m_j\}$ to determine if it is equal to d_{j+1} or d_n are performed in constant time using the implicit encoding of combinatorial pyramids [10].

2.3 Embedding of region boundaries

Let us consider the dart 16 in Fig. 1c. This dart encodes the border between the background and the first row of the 3×3 grid encoded by the σ_3 cycle $\sigma_3^*(16) = (16, 7, 8)$ of G_3. The sequence of initial darts encoding the boundary of the dart 16 is retrieved using Eq. (1) and is equal to: 16.15.14.13.24 (Fig. 1b). We have for example $15 = \varphi_0(\alpha_0(16)) = \varphi_0(-16)$ (Fig. 1c). Since each initial dart is associated to an oriented linel, one may associate a sequence of Freeman's code to each sequence of initial darts (Fig. 1b) and thus to each dart of a reduced combinatorial map G_i. The sequence of Freeman's codes associated to a dart d is denoted s_d and is called the *segment* associated to d. for example, the segment associated to the dart 16 is equal to $s_{16} = 1.2.2.2.3$.

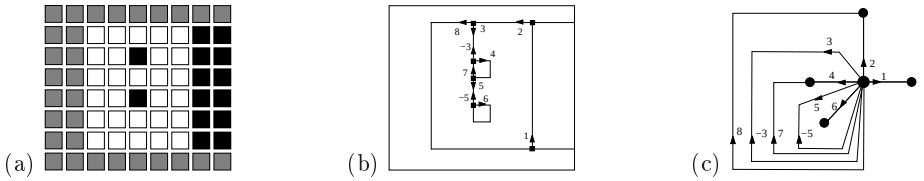

Fig. 2. The central white region $\sigma^*(1)$ (a) contains several subregions. Its boundary is thus split into several connected components connected by bridges in $\overline{G}$ (b). These edges correspond to self loops in G (c).

3 Discrete geometry over a partition

As mentioned in Section 2, each edge $(d, \alpha_i(d))$ of a partition G that is not a self loop encodes a connected boundary between two regions. The edge is called *separating*. On the other hand, a self loop corresponds to a bridge in the dual combinatorial map and is characterized by $\alpha_i(d) \in \sigma_i^*(d)$ (e.g. edge $(3, -3)$ or $(5, -5)$ in Fig. 2bc). Such edges, called *fictive*, either connect the outer boundary to some inner boundary (e.g. edge $(3, -3)$ in Fig. 2) or connect two inner boundaries (edge $(5, -5)$ in Fig. 2) [10].

Each separating edge is embedded as a 4-connected digital path, included in the interpixel digital plane (Section 2.3 and [10]). When estimating the geometry of the boundary of the region, fictive edges do not play any role. More precisely the concatenation of only the separating edges defines also a set of 4-connected digital loops. Each of these loops is either the outer boundary of the region or one of its inner boundaries [10]. Given an initial dart d belonging to a separating edge, Algorithm 1 extracts a boundary between region $\sigma^*(d)$ and its complement (setting $L_{\text{in}} = \sigma^*(d)$) or between regions $\sigma^*(d)$ and $\sigma^*(d')$ and their complement (setting $L_{\text{in}} = \sigma^*(d) \cup \sigma^*(d')$). Its principle is to follow the boundary with σ except it skips fictive edges and edges in-between $\sigma^*(d)$ and $\sigma^*(d')$. This method for tracking a boundary is easily understood on Fig. 2b, where for instance the algorithm tracks from dart 1, then $2 = \sigma(1)$, 3 is skipped since $-3 \in \sigma^*(1)$, then $8 = \sigma(-3)$ and terminates on $1 = \sigma(8)$ again. Extracting all the boundaries of a region is done in a similar way. All these algorithms can be implemented with a complexity linear with the number of boundary linels.

3.1 Geometry with digital straight segments

We may now examine how geometric quantities can be estimated on a closed 4-connected digital contour C, which is some boundary of a region or two adjacent regions (computed as in the previous paragraph). The literature is abundant on this topic and we restrict ourselves to pure discrete geometry tools based on *digital straight segment* (DSS) recognition. Several equivalent definitions of DSS exist together with several classes of algorithms to recognize them on digital curves (see for instance [12] for a recent survey). We chose here to present briefly the arithmetic point of view of digital lines, which leads to rather simple and efficient algorithms [13, 14].

Algorithm 1 Algorithm to visit all the linels of the digital boundary encircling region(s) specified by their darts L_{in} and containing the dart d.

```
1 Function Map::boundary( dart d, darts L_in ) : Freeman chain
Ensure: Return a sequence of Freeman's codes that is a 4-connected loop.
Require: d ∉ L_in
2 list C ← ∅,   dart b ←d
  repeat
    C.append(s_b)
    b ←σ(b)
    while α(b) ∈ L_in do {Skip fictive or interior edges}
      b ←φ(b)
    end while
  until b = d
  return C
```

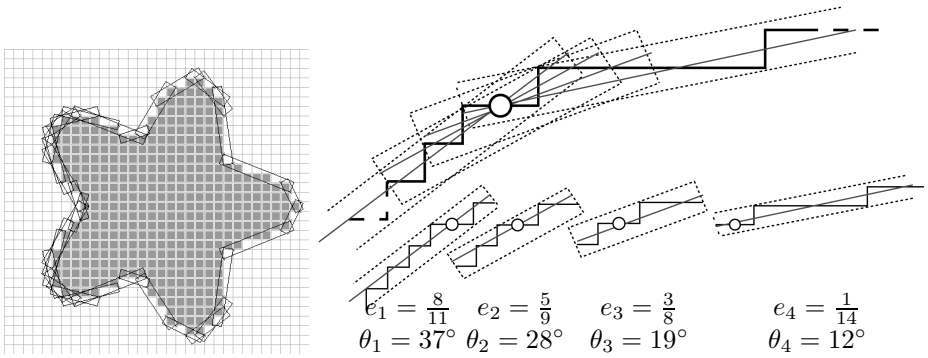

Fig. 3. Left: every maximal segment along this contour is drawn as its rectangular bounding box. Right: λ-Maximal Segment tangent estimation at a given point.

The set of points (x, y) of the digital plane verifying $\mu \leq ax - by < \mu + |a| + |b|$, with a, b and μ integer numbers, is called the *standard line* with slope a/b and shift μ. A standard line is always 4-connected. A sequence of consecutive points $C_{i,j}$ indexed from i to j of the digital curve C is a *digital straight segment (DSS)* iff there exists a standard line (a, b, μ) containing them. The one with smallest $a + b$ determines its *characteristics*, in particular its slope a/b. Any DSS Z thus defines an angle $\theta(Z)$ between its carrying standard line and the x-axis (in $[0; 2\pi[$ since a DSS is oriented), called the *direction of* Z.

The predicate *"$C_{i,j}$ is a DSS"* is denoted by $S(i, j)$. Incremental algorithms exist to recognize a digital straight segment on a curve and to extract its characteristics [13]. Therefore deciding $S(i, j + 1)$ or $S(i - 1, j)$ from $S(i, j)$ are $O(1)$ operations. Any DSS $C_{i,j}$ is called a *maximal segment* iff $\neg S(i, j + 1)$ and $\neg S(i-1, j)$. Maximal segments are thus the inextensible DSS of the curve (Fig. 3, left). Note that the set of all maximal segments of a curve can be computed in time linear with the number of curve points [14].

3.2 Tangent, normal and length estimation

Several tangent estimators based on DSS recognition have been proposed. We propose to use the λ-Maximal Segment Tangent estimator (λ-MST) to approach the tangent direction at any point of the digital curve [15]. It was indeed shown to give good approximations even at coarse scale, to be rather independent from rotations and to be asymptotically convergent.

Fig.3, right, gives the essential idea of this tangent estimator. Given a point, the direction θ_i of every maximal segment containing it is evaluated. The relative position e_i of the point within the maximal segment is also computed. The λ-MST tangent direction $\hat{\theta}$ is some weighted combination of the preceding parameters: $\hat{\theta} = (\sum_i \lambda(e_i)\theta_i)/(\sum_i \lambda(e_i))$. In our experiments, the mapping λ was defined as the triangle function taking base value 0 at 0 and 1, and peak value 1 at $\frac{1}{2}$. For further details, see [15].

The experimental average number of maximal segments per linel is between 3 and 4. Therefore computing the λ-MST direction is not costly and is a $O(1)$ operation on average. This technique of tangent estimation is easily extended to any real curvilinear abscissa along the digital contour. The tangent is thus defined at any linel, taking half integer abscissas.

The estimation of the *normal vector* at C_k is then simply the vector $\hat{\mathbf{n}}(k) = (-\sin(\hat{\theta}(k)), \cos(\hat{\theta}(k)))$. The *elementary length* $\hat{l}(k, k+1)$ of a linel $C_{k,k+1}$ is defined as $|\cos(\hat{\theta}(k+0.5))|$ for horizontal linels and $|\sin(\hat{\theta}(k+0.5))|$ for vertical linels. It corresponds to an estimation of the length of a unit displacement along the digital curve. The length of C is estimated by simple summation of the elementary length of its linels. This method of length evaluation was reported to give very good experimental results [16]. If C^b is boundary$(b, \sigma^*(b))$ as returned by Algorithm 1, then its *length* is $\hat{L}(b; G) = \sum_{k=1}^{|C^b|} \hat{l}(k, k+1; C^b)$. The total *perimeter* $\widehat{\mathrm{Per}}(R(\sigma^*(b)); G)$ of the region $\sigma^*(b)$ is the sum of the length of each of its boundaries.

4 Energy of a partition and pyramidal segmentation

The geometrical features (normal, perimeter, polygonalization) defined in Section 3 may be computed on each region of a partition in order to provide different measures of its geometrical characteristics. Such measures may then be incorporated into a hierarchical segmentation algorithm based on an energy minimization scheme (Section 1). Such energy balances two terms: the goodness of fit term and a regularization term which penalizes unlikely or complex models. The energy of a partition encoded by the map G is simply called the *energy of the combinatorial map* G and is formally defined as follows: Let $G = (\mathcal{D}, \sigma, \alpha)$ be a combinatorial map with a geometrical embedding in the digital grid and an input image I over this grid. Let $\mathcal{D}_\sigma$ be the set of σ-cycles of $\mathcal{D}$. The energy of the combinatorial map G is

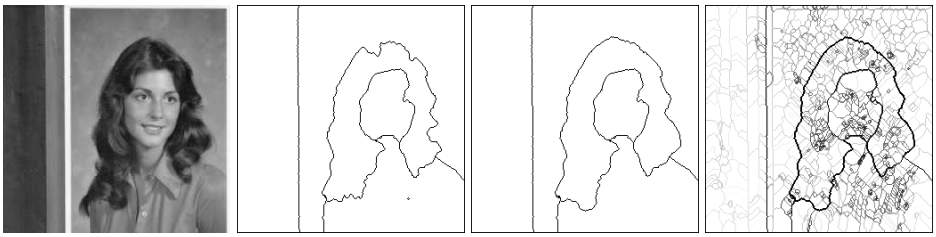

(a) (b) (c) (d)

Fig. 4. Influence of length penalization: (a) image Girl, (b) one level of the pyramid with $\hat{l}(k, k+1) = 1$, (c) same level of a pyramid built using discrete length estimators. All the boundaries of the pyramid which contains (c) are superimposed on (d). The darkest boundaries are those who survive at the highest levels.

$$E(G) = \sum_{\sigma^*(d) \in \mathcal{D}_\sigma} E(\sigma^*(d)) \quad (2) \qquad E(\sigma^*(d)) = E_{\text{img}}(\sigma^*(d)) + \nu E_{\text{reg}}(\sigma^*(d)) \quad (3)$$

Eq. (2) indicates that the global energy is decomposable over each region. This property helps in defining fast algorithms for region decimation. Eq. (3) balances the two energies, one dependent on the image (the image energy E_{img}), the other dependent only on the model (the regularization energy E_{reg}).

The parameter ν is often interpreted as a scale parameter, since it privileges the goodness of fit for low values (and over-segmentation) and *a priori* most likely regions for high values (and under-segmentation).

The image energy used within our experiments is defined as follows:

$$E_{\text{img}}(\sigma^*(d)) = -\delta \sum_{C_k \in C^d} \|D\ I(C_k)\| \hat{l}(k, k+1) + \sum_{(x,y) \in R(\sigma^*(d))} \|I(x,y) - \mu_{\sigma^*(d)}\|^2 \quad (4)$$

where $\hat{l}(k, k+1)$ denotes the length estimate of a lignel at point k, $I(x, y)$ denotes the color of the pixel (x, y) and $\|D\ I(C_k)\|$ the norm of the differential of I at point k. This last measure is equal to the norm of the gradient for grey level images. The term $\mu_{\sigma^*(d)}$ represents the mean color of the region encoded by $\sigma^*(d)$. The second sum of the above expression denotes thus the squared error of the region. Finally, the term δ represents the respective weight of the gradient and squared error energies.

The regularization energy is defined from the estimate of the perimeter of the region as $E_{\text{reg}}(\sigma^*(d)) = \widehat{\text{Per}}(R(\sigma^*(d)); G)$(Section 3.2). Given two possible merge operations inducing the same variation of the image energy, this choice for the regularization term favors the one which induces the simplest partition with the lowest overall length of contours. The advantage of using discrete length estimators compared to a basic count of the lignels is to make the segmentation process more independent on the alignment of components wrt some axes.

We tested the influence of length penalization on the classical Girl test image (Fig. 4). Two pyramids have been built on an initial partition encoded by a combinatorial map G_0. This partition is defined by a watershed algorithm applied on the gradient of the Girl test image. The parameter ν is fixed to 1.3 during the construction of both pyramids. Fig. 4(b) represent one level of the first pyramid built using a fixed length estimate equal to 1 for all lignels. Fig. 4(c), represents the same level within the second pyramid built using the discrete length estimator defined in Section 3.2. As shown by Fig. 4(c) the more accurate measure of the length given by the discrete length estimator provides smoothest boundaries.

Pyramidal segmentation algorithm

Our energy minimisation method starts with an initial partition coded by a map, and merges at each step the two adjacent regions, the merging of which induces the greatest decrease (or the smallest increase) of the combinatorial map energy. This process may be interpreted as a gradient descent which continues when a local minima is reached in order to seek for other minima. Note that our framework is not devoted to a specific strategy for energy minimization. Many alternative optimization heuristics could be used (e.g. the scale-climbing of Guigues *et. al.* [7]). The proposed approach is however sufficient to compare the respective advantages of different energies. Let us additionally note that using our strategy or the scale climbing of Guigues et al., only two regions are merged between two consecutive levels of the pyramid. This merge strategy does not induce a high memory cost due to the implicit encoding of the combinatorial pyramid [10]. An explicit construction of all the reduced graphs using graph or dual graph pyramids would require a huge amount of memory with a lot of redundancy between graphs.

5 Conclusion

We have presented a new framework for segmenting images with a pyramidal bottom-up approach using an energy-minimizing scheme. Our framework combines combinatorial pyramids, which can represent in the same structure all the levels of a hierarchy, and discrete geometric estimators, which provide precise geometric measurements and allow the definition of new regularization and image energy terms. A greedy algorithm for computing the hierarchy was also provided and some examples of segmentation were exhibited and discussed.

Our first experiments show that, the length estimation can have a great influence on the regularization of the segmentation. Discrete geometric estimators provides some smoothest boundaries. However, they are useless if the over-segmentation gives irregular regions. In futur works, we want to tackle this problem by using a smoothest over-segmentation.

References

1. Chan, T.F.: Active contours without edges. IEEE Transactions on image Processing **10**(2) (February 2001) 266–277
2. Leclerc, Y.G.: Constructing simple stable descriptions for image partitioning. International Journal of Computer Vision **3**(1) (May 1989) 73–102
3. Boykov, Y., Kolmogorov, V.: An experimental comparison of min-cut/max-flow algorithms for energy minimization in vision. IEEE Transactions on PAMI **26**(19) (2004) 1124–1137
4. Koepfler, G., Lopez, C., J.-M., M.: A multiscale algorithm for image segmentation by variational method. SIAM J. Numerical Analysis **31**(1) (1994) 282–299
5. Morel, J.M., Solimini, S.: Variational methods in image segmentation. Volume 14 of Progress in Nonlinear Differentiel Equations and Their Applications. Birkhäuser, Boston, Basel, Berlin (1995)
6. Reddings, N.J., Crisp, D.J., Tang, D.H., Newsam, G.N.: An efficient algorithm for mumford-shah segmentation and its application to sar imagery. In: Proc. Conf. Digital Image Computing Techniques and applications (DICTA). (1999) 35–41
7. Guigues, L., Cocquerez, J., Le Men, H.: Scale-sets image analysis. International Journal of Computer Vision, **68**(1) (2006.) 289 – 317
8. Jolion, J.M.: Data driven decimation of graphs. In Jolion, J.M., Kropatsch, W., Vento, M., eds.: Proceedings of 3^{rd} IAPR-TC15 Workshop on Graph based Representation in Pattern Recognition, Ischia-Italy (May 2001) 105–114
9. Kropatsch, W.G., Haxhimusa, Y., Lienhardt, P.: Hierarchies relating topology and geometry. In Christensen, H., Nagel, H.H., eds.: Proceedings of Cognitive Vision Systems (Seminar N° 03441 Dagstuhl). (2003)
10. Brun, L., Kropatsch, W.: Contains and inside relationships within combinatorial pyramids. Pattern Recognition **39**(4) (April 2006) 515–526
11. Lienhardt, P.: Topological models for boundary representations: a comparison with n-dimensional generalized maps. Computer-Aided Design **23**(1) (1991) 59–82
12. Klette, R., Rosenfeld, A.: Digital Geometry - Geometric Methods for Digital Picture Analysis. Morgan Kaufmann, San Francisco (2004)
13. Debled-Renesson, I., Réveillès, J.P.: A linear algorithm for segmentation of discrete curves. International Journal of Pattern Recognition and Artificial Intelligence **9** (1995) 635–662
14. Feschet, F., Tougne, L.: Optimal time computation of the tangent of a discrete curve: Application to the curvature. In: Proc 8th Int. Conf. Discrete Geometry for Computer Imagery (DGCI'99). Number 1568 in Lecture Notes in Computer Science, Springer Verlag (1999) 31–40
15. Lachaud, J.O., Vialard, A., de Vieilleville, F.: Analysis and comparative evaluation of discrete tangent estimators. In et al., E.A., ed.: Proc. Int. Conf. Discrete Geometry for Computer Imagery (DGCI'2005), Poitiers, France. Volume 3429 of LNCS., Springer (2005) 140–251
16. Coeurjolly, D., Klette, R.: A comparative evaluation of length estimators of digital curves. IEEE Trans. on Pattern Anal. and Machine Intell. **26**(2) (2004) 252–257